Magnetic-field-induced periodic deformations in planar nematic layers

D. Krzyżański* and G. Derfel
Institute of Physics, Technical University of Łódź, ulica Wólczańska 223, 93-005 Łódź, Poland
(Received 1 March 1999; revised manuscript received 16 November 1999)

Periodic deformations of strongly anchored planar nematic layers subjected to magnetic fields were studied numerically. Two magnetic-field configurations, giving rise to the so-called periodic splay-twist and periodic twist-splay patterns, were taken into account. The stationary director distribution was calculated for various values of elastic anisotropy and magnetic-field strength. Some alternative conclusions that shed light on the properties of the periodic deformations were drawn: (i) the transition from the periodically deformed structure to the homogeneously deformed one, which occurs in high field, is due to the divergence of the spatial period of the deformations to infinity; (ii) the spatial dependence of the angles determining the high-field director distribution strongly deviates from the theoretically predicted functions of sinusoidal form. The diagrams showing the ranges of parameters, for which the periodic deformations can realize, were built. The stable wave-number bands were determined numerically.

PACS number(s): 61.30.Cz, 61.30.Gd

I. INTRODUCTION

The career of liquid crystals is due to their permittivity to external fields. Due to the diamagnetic (dielectric) anisotropy of the liquid crystal, the magnetic (electric) field can influence the director distribution $\mathbf{n}(\mathbf{r})$ and thus change the optical properties of the layer. The influence of the field has been known since the early 1930s [1].

Let us consider the nematic liquid-crystal layer of thickness d placed between two plates parallel to the (x,y) plane in a Cartesian coordinate system. The most elementary field effect occurs in the planar layer in which the initial director $\mathbf{n}_0$, parallel to the x axis, is subjected to the perpendicular magnetic field $\mathbf{H}\|z$. The director distribution is given by the angle $\theta(z)$, measured between $\mathbf{n}$ and the (x,y) plane. The distortion is dominated by splay. This field effect is called the Fréedericksz transition. Other simple transition takes place in the planar layer if $\mathbf{H}\|y$. The director is uniformly twisted by the angle $\varphi(z)$ between the x axis and the projection of $\mathbf{n}$ on the (x,y) plane. The third elementary deformation with prevailing bend is realized in the homeotropic layer $(\mathbf{n}_0\|z)$ under the influence of the horizontal magnetic field; for instance, $\mathbf{H}\|x$. In all the mentioned geometries, the transition from the undistorted state (US) to the distorted one appears if the corresponding threshold field is exceeded. The director distribution along the z axis is identical throughout the whole area of the layer; thus the term homogeneous distortion (HD) is used. The angles θ and φ do not depend either on x or y.

The periodic distortions (PD's) are another, less common type of deformation. They can occur in all three of the geometries mentioned above (and in some modifications of them) if the elastic anisotropy is sufficiently large. They also possess the threshold character. The deformed director distribution is much more complicated. Both angles θ and φ are necessary for its description. The most distinguishing feature is spatial variation of these angles: in addition to their dependence on z, they change periodically along the y direction. The periodicity can be described by the wave vector $\mathbf{q}\|y$ or by the spatial period $\lambda=2\pi/q$ where $q=|\mathbf{q}|$. The periodic changes of director orientation imply the periodic changes of the optical properties of the layer, which are seen in a polarizing microscope as stripes.

The elastic periodic deformations arise in various liquid-crystalline systems. External fields can induce them in cholesterics [2–4] and in twisted nematics [5,6]. In the electric field, they are influenced by flexoelectric effects [7–9]. In addition to the stationary structures, the transient patterns following the applications of external field are observed, although the final distortion is homogeneous [10–12].

In this paper, we restrict our attention to the planar nematic layers influenced by magnetic fields. Positive diamagnetic anisotropy of the liquid crystal $\Delta\chi$ was assumed. In such layers, the PD's can take place in two basic cases: (i) when the field is perpendicular to the plane of the sample and (ii) when the field is parallel to the sample. In both cases the field is normal to the initial director. The periodic distortions in these geometries appear to be composed of splay and twist. In case (i), the splay distortion prevails; thus this kind of deformation is called periodic splay-twist (PST) deformation. In the second case, the twist deformation dominates, and the term periodic twist-splay (PTS) deformation is used. The PST deformations were first observed and theoretically analyzed by Lonberg and Mayer [13]. Later, their observations were followed by numerous theoretical analyses of PST and PTS deformations [2,8,14–20].

According to the theoretical findings concerning the planar nematic layer, reported in [14–17], a sufficiently large elastic anisotropy expressed by suitable values of the ratio $r=k_{22}/k_{11}$ is necessary for the occurrence of the periodic patterns. In the strongly anchored sample, the PST deformation can develop when r is lower than the limiting value $r_c \approx 0.3$. The patterns arise continuously when the free energy of the undistorted layer in the magnetic field becomes greater than the free energy of the periodically deformed layer. This condition determines the threshold strength of the magnetic field H_c. It is lower than the threshold for the Fréedericksz

*Author to whom correspondence should be addressed.

transitions [i.e., lower than $H_s=(\pi/d)\sqrt{k_{11}/\Delta\chi}$]. The difference H_S-H_c is proportional to $(r_c-r)^2$. The spatial period of the stripes λ increases with the field. Its value at the threshold is finite and proportional to $(r_c-r)^{-1/2}$. It means that λ tends toward infinity if $r\to r_c$, i.e., the periodic deformation disappears in this limit.

Analogous properties were found for the PTS patterns. They can arise if $r>r_c'=1/r_c\approx 3.3$. The threshold field H_c' is lower than the threshold for homogeneous twist deformation $H_T=(\pi/d)\sqrt{k_{22}/\Delta\chi}$ and depends on r according to the formula $(H_T-H_c')\propto(r-r_c')^2$. The spatial period λ diverges to infinity if r decreases to r_c', in agreement with $\lambda\propto(r-r_c')^{-1/2}$.

The director distribution in the periodically deformed layer was found for the PST case as a solution of the linearized torque equations [13,17]. The general form of this solution

$$n_y=g(z)\sin(qy),\qquad n_z=f(z)\cos(qy) \tag{1}$$

contains rather complex functions $f(z)$ and $g(z)$. A simplified description of director distribution can be given by means of functions

$$\theta(y,z)=\theta_m\cos(\pi z/d)\cos(qy),\qquad \varphi(y,z)=\varphi_m\sin(2\pi z/d)\sin(qy), \tag{2}$$

where θ_m and φ_m denote the amplitudes of the deformation [16,18]. For the PTS case the corresponding formulas read

$$\theta(y,z)=\theta_m\sin(2\pi z/d)\cos(qy),\qquad \varphi(y,z)=\varphi_m\cos(\pi z/d)\sin(qy). \tag{3}$$

In the present work, the structure of the stationary PST and PTS periodic deformations was studied by means of numerical simulations. The experimental recognition of the director distribution is rather difficult. A theoretical approach often involves the necessary simplification of assumptions, which may lead to results that are not only quantitatively but also qualitatively incorrect. Therefore computer simulations of the nematic layer subjected to the external field seem to be a valuable method, suitable for analysis of the director distribution in the layer, especially away from threshold.

Our numerical results, presented in the following, confirm some previous theoretical predictions. Nevertheless, alternative conclusions may be drawn from our analysis of the director distribution, which shed light on the problem of periodic deformations: (i) the PD-HD transition occurring in high field is due to the divergence of the patterns spatial period to infinity; (ii) $\theta(y,z)$ and $\varphi(y,z)$ dependencies, describing the high-field director distribution, cannot be approximated by functions of sinusoidal form.

In Sec. II the parameters of the system under investigation are specified and the method of the calculations is briefly described. The results are presented in Sec. III. Section IV is devoted to a short discussion.

II. METHOD

The calculations were performed for an infinite layer with strong planar boundary anchoring. The nematic liquid crystal was confined between two plates parallel to the (x,y) plane and positioned at $z=\pm d/2$. The initial director $\mathbf{n}_0$ was oriented along the x axis. The external magnetic field was directed either along the z axis (in the PST case) or along the y axis (in the PTS case). The positive diamagnetic anisotropy $\Delta\chi$ was assumed. The elastic properties were characterized by constant value $k_{33}/k_{11}=1.5$ and various ratios $r=k_{22}/k_{11}$. According to the results of experiments mentioned above, the stripes, which develop in this geometry, were directed along the x axis.

A single stripe of width λ was considered during the computations. The periodic boundary conditions along the y axis were imposed. The structure of the stripe was found by numerical minimization of the free energy per unit area of the layer. This quantity was expressed as the energy of the stripe, counted per unit length along the x axis, divided by the width λ.

The director distribution over the cross section of the stripe, described by the functions $\theta(y,z)$ and $\varphi(y,z)$, was approximated by discrete angles θ_{ij} and φ_{ij} defined in the sites of the $M\times N$ regular lattice. The indices $i=1,\ldots,M$ and $j=1,\ldots,N$ determined the position along the y and z axes, respectively. The coordinates $y=0$ and $y=\lambda$ were determined by $i=1$ and $i=M+1$. The sites placed at the boundary plates at $z=-d/2$ and $z=d/2$ were labeled by $j=1$ and $j=N$. Even M and odd N were used for convenience, due to the symmetry of the stripe. In most cases $M=32$ and $N=33$; at high fields, however, M was increased up to 64. The planes determined by $i=\text{const}$ and $j=\text{const}$ [parallel to the (x,y) and (x,z) planes, respectively] have divided the cross section of the stripe into $M\times(N-1)$ rectangular cells. The average angles θ and φ for each cell, as well as their spatial derivatives, were expressed by means of θ_{ij} and φ_{ij}. These values were used to calculate the elastic and magnetic free energy of the cell counted per unit length in the x direction. A sum of the energies related to all the $M\times(N-1)$ cells divided by λ was equal to the total free energy per unit area of the layer.

Initially, the values $\theta_{ij}=0$ and $\varphi_{ij}=\pi/2$ for all i and j, and the ratio $\lambda/d=1$ were imposed. To start the deformation, a small deviation from the initial director position at one arbitrarily chosen site of the lattice was introduced. The final set of the θ_{ij} and φ_{ij} and λ/d variables, which approximated the real equilibrium director distribution, was calculated in the course of an iteration process. During the computations, these variables were varied successively by small intervals. The angles with indices $(i,1)$ and (i,N) could remain unchanged according to the rigid boundary conditions. The free energy per unit area of the layer was calculated after each change. New values of the variables were accepted if they led to the lower free energy. This procedure was repeated until no further reduction in the total free energy could be achieved. Then the interval was decreased and the process repeated. As a result, a state with minimum energy was obtained. The resulting discrete director distributions possessed interesting symmetry properties—the same as the symmetry due to the theoretical solution given by Eqs. (2) and (3).

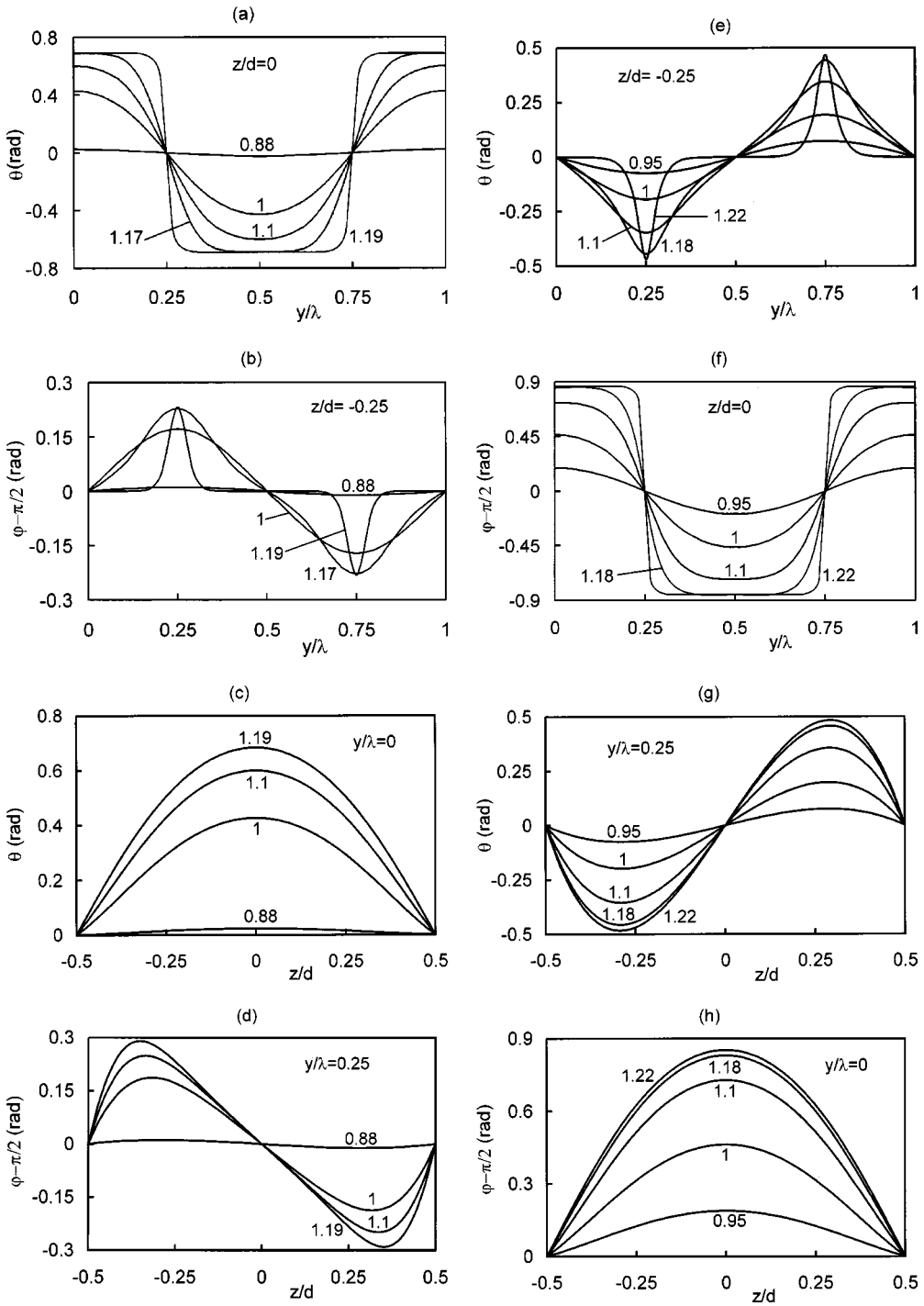

FIG. 1. The director distribution within a single stripe illustrated by means of $\theta(y/\lambda)$, $\varphi(y/\lambda)$, $\theta(z/d)$, and $\varphi(z/d)$ functions plotted for various magnetic-field ratios as indicated: (a)–(d) PST, $r=0.15$; (e)–(h) PTS, $r=5$.

Therefore we used this symmetry in order to accelerate the calculations by computing the director distribution only in one-eighth of the stripe cross section, i.e., for $i=1,\ldots,M/4$ and $j=1,\ldots,N/2+1$. The results were suitably copied for the rest of the stripe.

The free-energy minimization procedure was performed for different k_{22}/k_{11} and H/H_S (or H/H_T) ratios. The set of angles obtained in this way for some set of parameters of the system served as a starting point to computations for other parameters. This procedure was created in analogy to the method developed earlier in [21]. It was applied to various one- and two-dimensional deformations of nematic layers [21,22].

III. RESULTS

In the following, the main features of the periodic deformations, revealed by the numerical computations, will be described. We present them simultaneously for the PST and PTS cases, in order to show the similarity between these two modes of deformation.

The structure of a single stripe is illustrated by means of

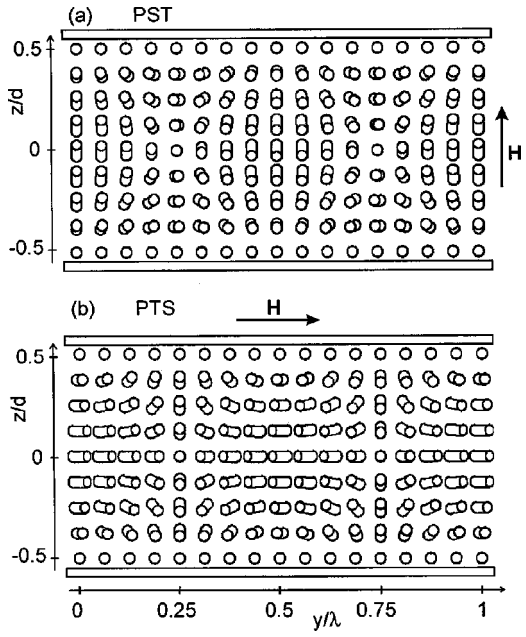

FIG. 2. The schematic representation of the director field within a single stripe: (a) PST, (b) PTS.

functions $\theta(y/\lambda)$, $\varphi(y/\lambda)$, $\theta(z/d)$, and $\varphi(z/d)$, plotted for representative cross sections of the layer and for various magnetic-field strengths. Figures 1(a)–1(d) concern the PST case and Figs. 1(e)–1(h) exemplify the PTS case. The curves are sinusoidal only at low fields. Their shapes at high fields are remarkably different. In particular, the y dependencies of the angles θ in the PST case and φ in the PTS case show the existence of significant regions with almost uniform deformation of opposite signs within two halves of the stripes.

The periodic features of the director distribution illustrated by the plots in Figs. 1(a)–1(h) can be summarized as follows. When we move parallel to the y axis, we observe

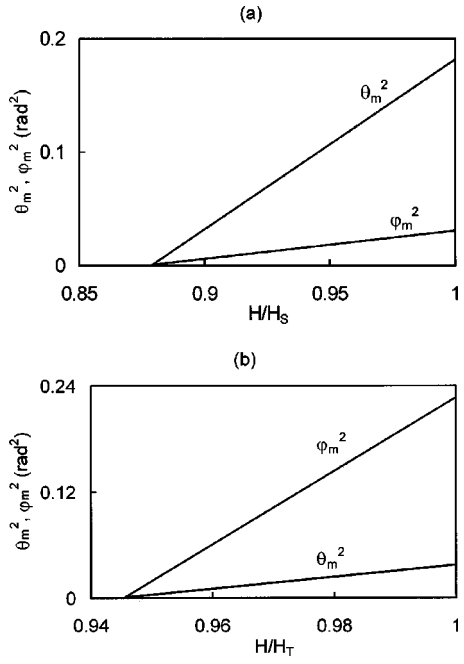

FIG. 3. Squares of the amplitudes θ_m and φ_m plotted as functions of H/H_S (or H/H_T) ratios: (a) PST, $r=0.15$; (b) PTS, $r=5$.

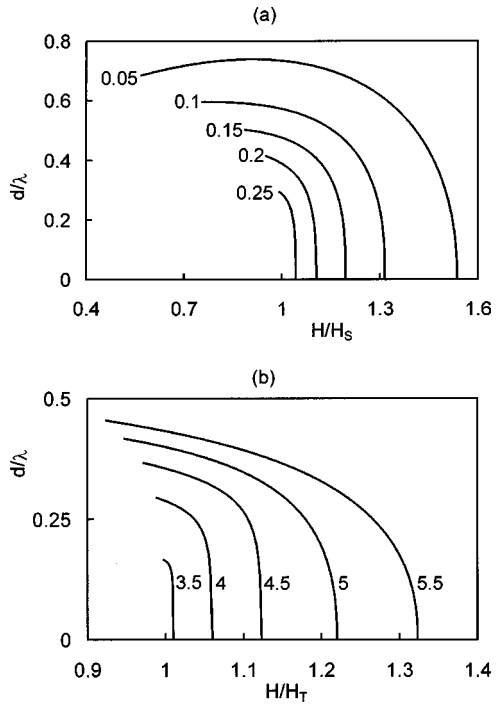

FIG. 4. The dependence of the reversed spatial period on the magnetic-field strength for several values of elastic anisotropy: (a) PST, (b) PTS; the values of r are indicated for each curve.

that the director rotates around the x axis and is confined to the surface of a cone with an oval base. By moving parallel to the z axis, similar rotation is observed, but the axis of the cone deviates from the x direction. The vertex angles of the cones increase with the field. The base of the cone is reduced to a straight line if the director variation in the midplane $z/d=0$, or in the planes $y/\lambda=0$, $y/\lambda=0.25$, $y/\lambda=0.5$, and

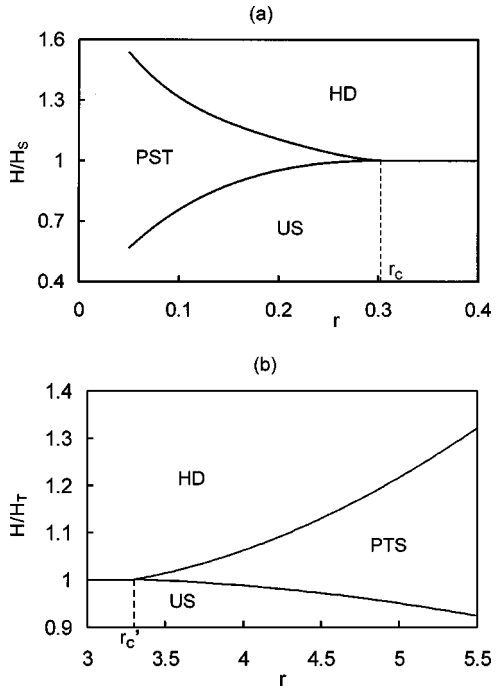

FIG. 5. The ranges of existence of the periodic deformations: (a) PST, (b) PTS.

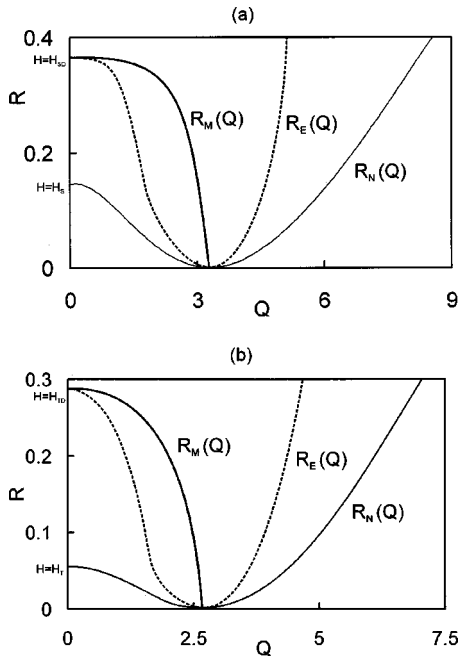

FIG. 6. Stability boundaries for the periodic deformations: (a) PST, $r=0.15$; (b) PTS, $r=5$; $R_M(Q)$—free-energy minimizing wave numbers; $R_N(Q)$—neutral stability curves; $R_E(Q)$—Eckhaus-stability boundaries.

$y/\lambda=0.75$, is considered. Figures 2(a) and 2(b) show the stripes' structures schematically by means of cylinders that symbolize the director.

Figures 3(a) and 3(b) illustrate the PD development at low fields by means of amplitudes θ_m and φ_m plotted as functions of H/H_S (or H/H_T) ratios. The second-order character of the HD-PD transition at $H=H_c$ (or $H=H_c'$) is revealed. Both angles are proportional to $[(H-H_c)/H_S]^{1/2}$ in the PST case and to $[(H-H_c')/H_T]^{1/2}$ in the PTS case. Dependence of this type is well known for the homogeneous deformations. From Figs. 1 and 3 it is evident that the roles of the angles θ and φ in the PST and PTS modes are interchanged, as was noticed in [18] and [20].

The initial width of the strip λ was comparable with the layer thickness. Its value was proportional to $(r_c-r)^{-1/2}$ and $(r-r_c')^{-1/2}$ in the PST and PTS cases, respectively, in agreement with the theoretical predictions mentioned earlier.

The dependence of the spatial period on the magnetic-field strength for several values of elastic anisotropy is illustrated in Figs. 4(a) and 4(b) by the plots of d/λ versus H/H_S and H/H_T, respectively. In general, the period increases with the field, in agreement with the experimental observations [13]. However, in the PST case, when the elastic anisotropy was particularly high ($r=0.05$), a slight decrease of λ was observed at low fields. This effect was not found in the PTS case. At some critical field H_{SD} (H_{TD}), the period λ diverges to infinity. With an infinite increase of λ, the single stripe spreads over the whole layer. This is equivalent to the transition to homogeneous deformation.

The ranges of the field strength, in which the PD can arise, expressed by $H_{SD}-H_c$ and $H_{TD}-H_c'$, depend on the k_{22}/k_{11} ratio. They become narrower when the k_{22}/k_{11} ratio tends toward r_c (or r_c'). The ranges of existence of the periodic deformations in the $(r,H/H_S)$ and $(r,H/H_T)$ planes are shown in Figs. 5(a) and 5(b).

IV. DISCUSSION

In this paper, we present the results of the numerical calculations concerning the stationary director distribution in the periodic distortions induced by a magnetic field in a planar nematic layer. The main qualitative properties of our solutions agree with the experimental data. Nevertheless some different features have been revealed.

It was found that the functions describing the spatial dependence of the angles θ and φ are sinusoidal only for the field strengths very close to the corresponding threshold values. Therefore the theoretical predictions, based on the linearized torque equations yielding such types of y dependence, are only valid in rather narrow regions of the sufficiently low fields. In the high field, the orientations within prevailing parts of two halves of a stripe become almost independent of y, i.e., the almost homogeneously deformed structures arise. They are separated by relatively thin walls of strongly deformed material. We have also calculated the high-field director profiles in the HD structures, and found that the functions $\theta(z)$ in the $\mathbf{H}\|z$ case and $\varphi(z)$ in the $\mathbf{H}\|y$ case were very close to the corresponding functions obtained for the homogeneously deformed parts of stripes in the PST and PTS cases, respectively. This comparison indicates the equivalence of the HD structures and the quasihomogeneous regions in the stripes. When the stripes broaden in the increasing field, their homogeneously deformed regions spread over a large distance across the layer. When λ is comparable with the size of a finite layer, this process can lead to the transition from PD to HD. The divergence of λ to infinity resembles the unwinding of the cholesteric helix during the field-induced cholesteric-nematic transition [23], when the pitch tends toward infinity with the field approaching some critical value. This analogy strongly supports our results concerning the PD-HD transition.

The periodic deformations described in this paper can be considered as an interesting example of a wide class of pattern-forming phenomena [24]. Nematic liquid-crystal layers are well-known systems in which pattern formation has been intensively investigated, mainly by studies of electrohydrodynamic instabilities (electroconvection) [25] and, to a lesser extent, by studies of Rayleigh-Bénard convection [26] and oscillatory shear instabilities [27]. The PST deformations may have some influence on the electroconvection [25]. A smooth transition between electrohydrodynamic instabilities and PST was predicted [28].

The PST and PTS deformations reveal many features usually observed for other pattern-forming systems. According to the classification given in [24], they belong to the I_s type; i.e., they are periodic in space and stationary in time, with a continuous band of wave vectors $\mathbf{q}$. We have determined the width of the stable wave-number band, which is one of the important problems in the field of pattern formation.

The magnetic field of strength H applied to the layer plays the role of the control parameter. The examples of the wave-number bands are presented in Figs. 6(a) and 6(b), in the (R,Q) plane, where $R=(H-H_c)/H_c$ (in the PST case) or $R=(H-H_c')/H_c'$ (for the PTS patterns) is the reduced field

strength and $Q=qd$ is the dimensionless wave number. The periodic deformations appear if the planar structure becomes unstable against small periodic perturbations. A stationary periodic pattern is formed through a continuously arising instability with finite q. The liquid-crystal layer, deformed by an external field, forms a gradient system for which the free-energy density per unit area F can be treated as the potential. For a given sample subjected to a given field, this potential is functional of the $\theta(y,z)$ and $\varphi(y,z)$ functions, and as a consequence it also depends on q. Actually stable periodic states with the wave number q_0 correspond to the minima of this functional. They are represented by the plots $R_M(Q)$, which are the suitably rescaled inverse functions $d/\lambda=f(H/H_S)$ and $d/\lambda=f(H/H_T)$, shown in Figs. 4(a) and 4(b). In each case the patterns set in at $q=q_c$ correspond to the threshold field strength H_c (or H_c').

There is a continuous band of wave numbers in the vicinity of q_0 for which the free energy of the periodic states is lower than that of the undeformed state. These states are limited by the neutral stability curve $R_N(Q)$. The free energy is zero at this limit. The periodic states above the neutral curve are energetically more favorable than those in the undeformed layer. Below the linear stability curve, a small periodic deformation will decay. The amplitude of the periodic structure vanishes continuously at the neutral curve. This property was used to obtain the function $R_N(Q)$. The amplitudes θ_m and φ_m were calculated as functions of Q, and the limiting Q values were determined by extrapolation $\theta_m\rightarrow 0$ and $\varphi_m\rightarrow 0$. The left branch of the neutral curve ends at $q=0$ and $H=H_S$ (or $H=H_T$), which reflects the fact that above this threshold field the zero-wave-number structure (i.e., the homogeneously deformed one) becomes energetically more advantageous than the undeformed state (however, it remains unstable with respect to the periodic deformations). The same shape of the stability limit was presented in [5] for another type of PD found in twisted nematic layers.

The periodic pattern whose wave number is too far from the minimizing value q_0 becomes unstable with respect to modulations called Eckhaus instability. This perturbation first occurs as a distortion over arbitrarily long length scales. The Eckhaus-stability criterion for potential systems is given by $\partial^2 F/\partial Q^2>0$ [29]. The curves $R_E(Q)$ in Figs. 6(a) and 6(b) show the limits of the corresponding stability. In order to find them, the inflection points of the functions $F(Q)|_{H=\text{const}}$ were determined numerically. Above the $R_E(Q)$ curve, the periodic states are resistive to the Eckhaus instability. In the vicinity of the critical field H_c (or H_c'), both neutral curve $R_N(Q)$ and Eckhaus curve $R_E(Q)$ are nearly parabolic, and the universal rule $R_E(Q)=3R_N(q)$ is well obeyed. The left branch of each Eckhaus line approaches the minimum-energy curve $R_M(Q)$ and joins it at $q=0$ and $H=H_{SD}$ (or $H=H_{TD}$). This corresponds to the fact that the homogeneously deformed states become stable above this critical field.

It should be noted that the deformations in unrestricted geometry considered here are different from the finite layer case, where the problem of selection of the wave numbers arises [24]. For infinite systems the limits of existence of periodic solutions are determined by bulk properties. Boundaries act to reduce the full band allowed by the bulk.

[1] V. Fréedericksz and V. Zolina, Trans. Faraday Soc. **29**, 919 (1933).
[2] P. Schiller, Phase Transit. **29**, 59 (1990).
[3] P. Schiller and K. Schiller, Liq. Cryst. **8**, 553 (1990).
[4] P. Schiller, Mol. Cryst. Liq. Cryst. **180B**, 177 (1990).
[5] V. I. Tsoy, G. V. Simonenko, and V. G. Chigrinov, Liq. Cryst. **13**, 227 (1993).
[6] U. D. Kini, J. Phys. (France) **48**, 1187 (1987).
[7] L. K. Vistin, Dokl. Akad. Nauk SSSR **194**, 1318 (1970) [Sov. Phys. Dokl. **194**, 908 (1971)].
[8] P. Schiller, G. Pelzl, and D. Demus, Cryst. Res. Technol. **25**, 111 (1990).
[9] Yu. P. Bobylev and S. A. Pikin, Zh. Éksp. Theor. Fiz. **72**, 369 (1977) [Sov. Phys. JETP **45**, 195 (1977)].
[10] B. L. Winkler, H. Richter, I. Rehberg, W. Zimmermann, L. Kramer, and A. Buka, Phys. Rev. A **43**, 1940 (1991).
[11] A. J. Hurd, S. Fraden, F. Lonberg, and R. B. Meyer, J. Phys. (France) **46**, 905 (1985).
[12] A. Buka and L. Kramer, Phys. Rev. A **45**, 5624 (1992).
[13] F. Lonberg and R. B. Meyer, Phys. Rev. Lett. **55**, 718 (1985).
[14] C. Oldano, Phys. Rev. Lett. **56**, 1098 (1986).
[15] W. Zimmermann and L. Kramer, Phys. Rev. Lett. **56**, 2655 (1986).
[16] G. Derfel, Liq. Cryst. **11**, 431 (1992).
[17] E. Miraldi, C. Oldano, and A. Strigazzi, Phys. Rev. A **34**, 4348 (1986).
[18] U. D. Kini, Mol. Cryst. Liq. Cryst. **153**, 1 (1987).
[19] A. Sparavigna and A. Strigazzi, Mol. Cryst. Liq. Cryst. **254**, 209 (1994).
[20] G. Barbero, E. Miraldi, and C. Oldano, Phys. Rev. A **38**, 519 (1988).
[21] S. E. Bedford, T. M. Nicholson, and A. H. Windle, Liq. Cryst. **10**, 63 (1991).
[22] G. Derfel, in *Liquid Crystals: Material Science and Applications*, edited by J. Zinija, Z. Raszewski, and J. Zielinksi, special issue of Proc. SPIE **2372**, 143 (1995).
[23] P. de Gennes, Solid State Commun. **6**, 163 (1968).
[24] M. C. Cross and P. C. Hohenberg, Rev. Mod. Phys. **65**, 851 (1993).
[25] L. Kramer and W. Pesch, in *Pattern Formation in Liquid Crystals*, edited by A. Buka and L. Kramer (Springer-Verlag, New York, 1995).
[26] P. J. Barratt, Liq. Cryst. **4**, 223 (1989).
[27] E. Dubois-Violette, G. Durand, E. Guyon, P. Manneville, and P. Pierański, in *Liquid Crystals*, special issue of Solid State Phys. (Tokyo) **14**, 147 (1978).
[28] E. Bodenschatz, W. Zimmermann, and L. Kramer, J. Phys. (France) **49**, 1875 (1988).
[29] L. Kramer and W. Zimmermann, Physica D **16D**, 221 (1985).